International Journal of Civil Engineering (IJCE)
ISSN(P): 2278-9987; ISSN(E): 2278-9995
Vol. 3, Issue 2, Mar 2014, 7-14

International Academy of Science, Engineering and Technology
Connecting Researchers; Nurturing Innovations

A PROFOUND MICROSCOPIC STUDY ON GEOPOLYMER CONCRETE

A. RANGANATHAN[1] & R. MALATHY[2]

[1]Department of Public Works, IHH, Chennai, Tamil Nadu, India

[2]Sona College of Technology, Salem, Tamil Nadu, India

ABSTRACT

The alkali activation of waste materials like fly ash has become an important area of research because it is possible to use these material to synthesize inexpensive and ecologically sound cement like construction materials. In this paper, the mechanism of activation of a fly ash with highly alkaline solution is described. These solution made with NaOH and Na_2SiO_3 having the common characteristics of having a very high OH^- concentration. Owing to their high strength and predominantly amorphous microstructure the materials on the basis of latent hydraulic active substances activated by alkalis like flyash and therefore, they are included into the group of so-called "chemically bonded products". The new eco friendly concrete being formed during the polymerisation of fly ashes exhibit their amorphous character with minority crystalline phases.

KEYWORDS: Alkaline Liquid, Fly Ash, Geopolymer Concrete, SEM, X-Ray Diffraction

INTRODUCTION

Geopolymer concrete that utilizes waste material containing silica (Si) and Alumina (Al) such as fly ash is a good alternative because it has a very low rate of green house gas emissions compared to OPC concrete. In geopolymer concrete, the silica and the alumina present in the source materials are first induced by alkaline activators to form a gel. This geopolymer gel binds the loose aggregates and other unreacted materials in the mixture to form the geopolymer concrete. The chemical process involved in the formation of geopolymer binders is very different to that of OPC concrete. The advent od advanced instrumental techniques, such as SEM analysis and X-ray Diffraction method are conducted to clarify important aspects of the structure and morphology of these new materials.

A Scanning Electron Microscope (SEM) is a type of electron microscope that produces images of a sample by scanning it with a focused beam of electrons. The electrons interact with electrons in the sample, producing various signals that can be detected and that can contain information about the sample's surface topography and composition. The electron beam is generally scanned in a raster scan pattern, and the beam's position is combined with the detected signal to produce an image. SEM can achieve resolutions better than 1 nanometer. Specimens can be observed in high vacuum and low vacuum and environmental SEM specimens can be observed in wet condition.

X-ray scattering techniques are a family of non-destructive analytical techniques which reveal information about the crystal structure, chemical composition, and physical properties of materials and thin films. These techniques are based on observing the scattered intensity of an X-ray beam hitting a sample as a function of incident and scattered angle, polarization, and wavelength or energy. The X-Ray Diffraction (XRD) analysis was conducted to ascertain the silica phase of the geopolymer concrete sample. In this analysis, firstly the specimens were scanned by an X-ray diffractometer using CuKα radiation at 40kV / 20 mA, CPS = 1 k, width 2.5, speed 2° / min and scanning with an angle of 2 Theta from

10° to 80°. In X-ray diffraction, X-rays were scattered by atoms in a pattern that indicated lattice spacings of elements present in the specimen and analyzed. When the X-rays are in phase, they will give constructive interference and produce a wavelength peak in the X-ray diffraction pattern. The wavelength of the X-rays are measured over a wide range of angles, and then the spacing of the material was found out.

EXPERIMENTAL

The micro structural experiments were carried out with a fly ash and geopolymer concrete.

Scanning Electron Microscope: Back—Scattered Electrons (BSE) are beam electrons that are reflected from the sample by elastic scattering. BSEs are often used in analytical SEM along with the spectra made from the characteristic X-rays, because the intensity of the BSE signal is strongly related to the atomic number (Z) of the specimen. BSE images can provide information about the distribution of different elements in the sample. In this investigation, fly ash sample, OPC and GPC samples which had been tested at 28 days for compressive strength were broken into small specimens and pulverized into powder form and sealed in air tight zip lock bags for further investigation. The specimens were then prepared and tested on a SEM (Scanning Electron Microscope) in order to make a qualitative assessment of the micro structure. The scanning electron microscope is a very useful tool for monitoring the micro structural development of the fly ash and the geopolymer concrete matrix specimen.

X-Ray Diffraction: This process of making out a qualitative assessment of the elements and the compounds present in the substance were analyzed. The specimen samples of low calcium fly ash and geopolymer concrete were analyzed using the X-ray diffractometer. A small amount of specimen sample in the form of powder was put into an aluminium sample holder and the surface was smoothed. The sample holder was then placed into the X-ray diffractometer and analyzed from 2 Theta angles of 10° to 80°. The analysis was carried out at 0.04 degree increment and timed for a period of 3 seconds. The results from X-ray diffraction analysis exhibited a number of minerals present in the samples. Each sample was analyzed with its peak intensities found for the individual angles from the database.

RESULTS AND DISCUSSIONS

The SEM images of fly ash powder with different magnifications are shown in Figures 1 Figure 1(a) is a micrograph showing the magnified image of fly ash with 200 magnifications. It shows a series of spherical and vitreous particles of diameters ranging from 9 µm to 82 µm. The scale bar is 100 µm. Figure 1(b) is a micrograph showing the magnified image of fly ash with 500 magnifications. It displays the size of the fly ash particles that range from 4 µm to 35 µm. The shape of the particles is spherical and the scale bar is 50 µm. Figure 1(c) is a micrograph that shows the magnified image of fly ash with 700 magnification. It indicates the spherical shaped fly ash particles ranging between 2.5 µm and 32.5 µm. The scale bar is 20 µm. Also, Figure 1(d) is a micrograph profiling the magnified image of the fly ash with a higher magnification, i. e. 1000 magnification. It shows the size, that is the diameter of fly ash particles ranging from 7.5 µm to 35 µm and the scale bar is 10 µm.

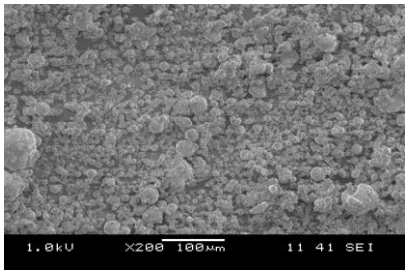

(a) Fly Ash with 200 Magnification

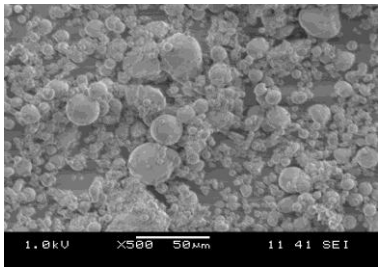

(b) Fly Ash with 500 Magnification

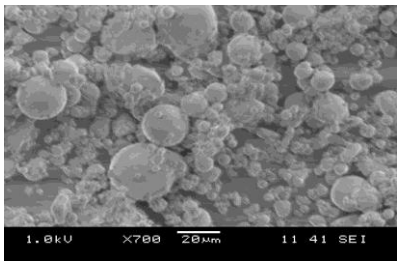

(c) Fly Ash with700 Magnification

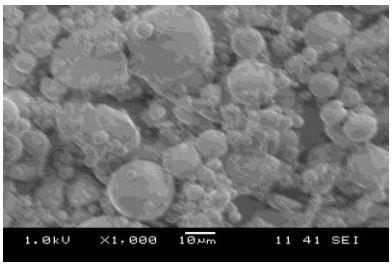

(d) Fly Ash with 1000 Magnification

Figure 1: SEM Images of Fly Ash

From these micrographs 1(a) to 1(d), it is observed that SEM images delineate the characteristic morphology of the original fly ash. It is found that this fly ash consists of a series of spherical and vitreous particles of different sizes, ranging from 7.5 µm. to 35 µm. The fly ash particles are usually hollow and some of these spheres may contain other particles of a smaller size in their interiors. Also, the spherical shape of fly ash facilitates the formulation of a simple conceptual mix, capable of describing the general process of the alkali activation of the ash. It is observed that almost all fly ash is activated resulting in a dense paste.

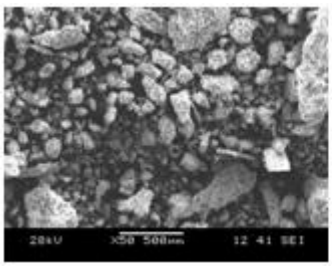

(a) OPC 20

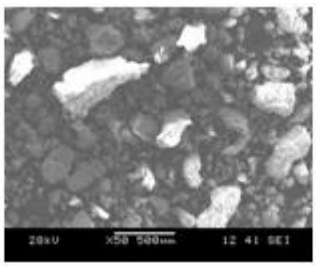

(b) OPC 30

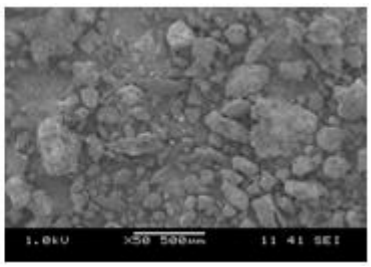

(c) OPC 40

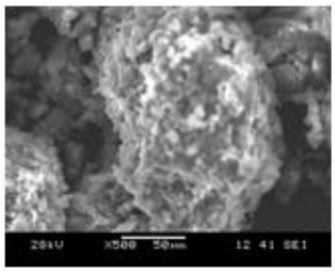

(d) GPC 20

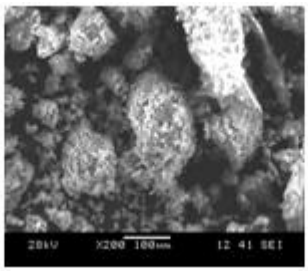

(e) GPC 30

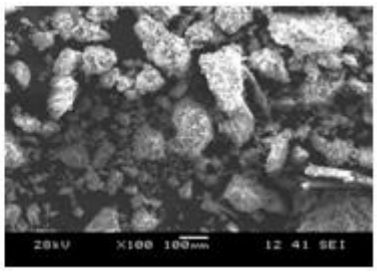

(f) GPC 40

Figure 2: SEM Images of OPC and GPC for Various Grades

Figure 2 illustrates the microstructure image of ordinary port land cement concrete and geopolymer concrete sample for various grades such as M20, M30 and M40. It also highlights the scale bar details and magnification factor of each grade of OPC and GPC. Figure 2 (a) consists of the SEM image of OPC of grade 20 with 50 magnification. It portrays

the irregular shaped particles whose lateral dimension ranged from 100 µm to 400 µm and its length varied from 400 µm to 1200 µm. The scale bar is 500 µm. These particles contain more voids between each particle. Figure 2 (b) is a micrograph that indicates the magnified image of OPC of grade 30 with 50 magnification. The image shows the rectangular shaped particle and some of them are irregular shaped. The size of the particles varied from 20 µm to 145 µm in width and 62 µm to 790 µm in length. The scale bar is 500 µm. Also, from the micrograph of OPC 30, it is observed that the concrete paste is not so dense. In fact, it is a little porous.

Figure 2(c) is a micrograph that indicates the magnified image of OPC of grade 40 with 50 magnification. The image manifests the irregular shaped particle. The size of the particles varied from 15 µm to 150 µm in diameter. The scale bar is 500 µm. Also, from the micrograph of OPC 40, it is observed that the concrete paste is loosely packed. Figure 2 (d) consists of the SEM image of GPC of grade 20 with 500 magnifications. The image clarifies that the particles are more thickly bonded and it forms a thick layer due to the well polymerization of alkaline liquids with fly ash. The size of the particles varied from 15 µm to 160 µm in diameter. The scale bar is 50 µm. Also, from the micrograph of GPC 20, it is observed that the concrete paste is densely packed.

Figure 2 (e) expresses the SEM image of GPC of grade 30 with 200 magnification. The image shows that the particles are more viscous and it forms a cluster of thick threaded paste. The size of the particles varied from 20 µm to 170 µm in diameter. The scale bar is 100 µm. Also, from the micrograph of GPC 30, it is observed that the concrete paste is more densely packed than GPC 20 mix. Figure 2 (f) is a micrograph that indicates the magnified image of GPC of grade 40 with 100 magnification. The image shows the particles are so compact and highly viscous and the particles are irregularly shaped. The size of the particles varied from 15 µm to 140 µm in width. The scale bar is 500 µm. Also, from the micrograph of OPC 40, it is observed that the concrete paste is closer and denser than GPC 20 and GPC 30 grade mixes.

Figure 2 reveals that the particles of geopolymer concrete are irregularly shaped but very compact. In this geopolymer concrete, the continuity of the mass of reaction product appears like a layer of viscous fluid, suddenly frozen indicating the complete polymerization process. The activation reaction rate, as well as the chemical composition of these products, depends on several factors like the particle size distribution, mineral composition of the fly ash and penetration of the activator. The specimen belongs to the fly ash paste, which is activated by using sodium silicate and sodium hydroxide solution. Then it is thermally cured at 90^0C for 72 hours. The developed microstructure of the geopolymer concrete looks very much like a uniform and unshaped microstructure.

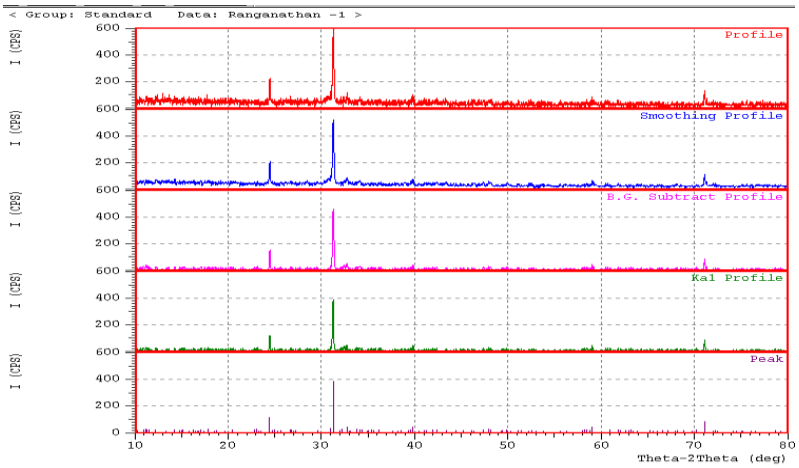

Figure 3: X-Ray Diffraction Pattern of Low Calcium Fly Ash

Figure 3 represents the X-ray diffraction pattern of low calcium fly ash sample. In this method, the 2θ angle is on abscissa and the intensity of mineral is plotted along ordinate. The graph contains the 2θ angle in the range of 0 to 600. The intensity is represented in counts. The X-Ray Diffraction (XRD) analysis was conducted to determine the silica phase of the given sample. This process ensured a qualitative determination of the elements and the compounds present in the sample. From the X-ray diffraction result, it is clear that there are a number of minerals present in the sample. The observed minerals were silica, calcium, alumina and oxides. The mineral found in this fly ash sample was Quartz with low intensity. The crystalline system was Hexagonal and the lattice was primitive. The molecular weight of mineral was 60.08.

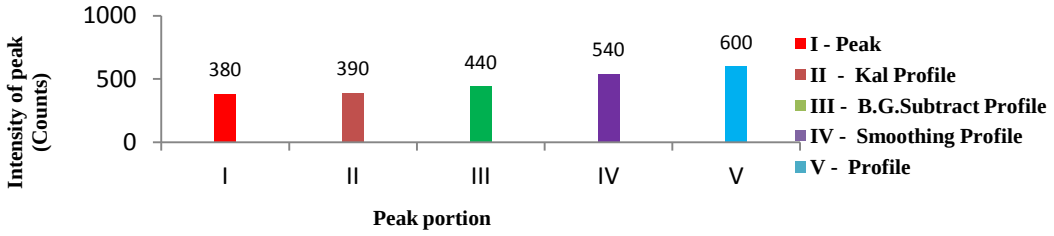

Figure 4: Intensity of Silicon Oxides in Fly Ash Sample

From the various portions of XRD graph, the intensity of silicon oxide of fly ash sample is plotted in a graph which is shown in Figure 4. From Figure 4, it is evident that the intensity of silicon oxide content of fly ash is ranging from 380 counts to 600 counts. The V-profile shows the intensity of silicon oxide of about 60% more than the I-peak intensity. Also, the V-profile has 55% and 37% higher than the II-Kal profile and III-B. G. subtract profile intensities. Similarly, the V-profile has 11% increased value than IV-smoothing profile intensity. From these observations, it is realized that the silicon content intensity gradually increased and it attained maximum at the profile portion only.

Figure 5 presents the X-ray diffraction pattern of the geopolymer concrete powder. It confirms that the peak represented the presence of sodium hydroxide and sodium silicate material in the concrete powder. According to the X-ray data, when the fly ash was activated with solutions of sodium silicate and sodium hydroxide, the material did not contain any crystalline phase. Thus the whole samples, studied by means of XRD, contained an amorphous component.

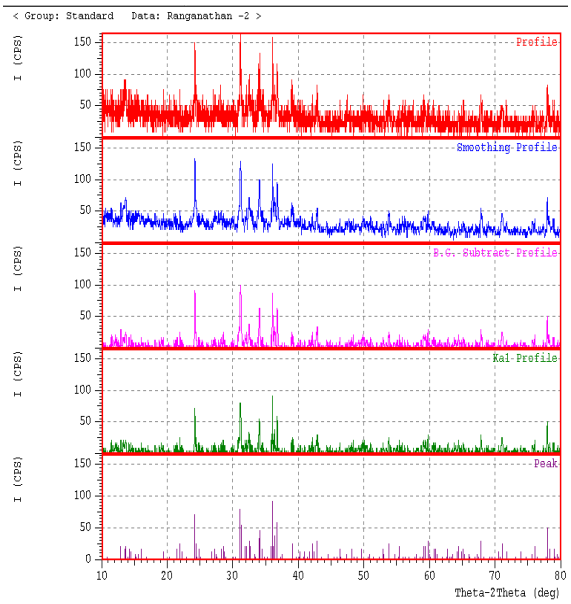

Figure 5: X-Ray Diffraction Pattern of Geopolymer Concrete

Figure 5 illustrates the X-ray Diffraction pattern of geopolymer concrete sample. The graph contains 2θ angle in the range of 10° to 80° and the intensity is in the range of 0 to 150 counts. In this graph, the mineral NaOH was identified more in crystalline form. The crystalline system was orthorhombic. The lattice was end-centered. The molecular weight of mineral was 40.00 with its volume (CD) = 131.47 with D_x = 2.021. NaOH was present in crystalline form due to the peak at 2θ angle of 31°, 34° and 37°. These peaks denoted the sodium hydroxide content in its crystalline nature and many other small peaks denoted other oxide compounds present in the sample.

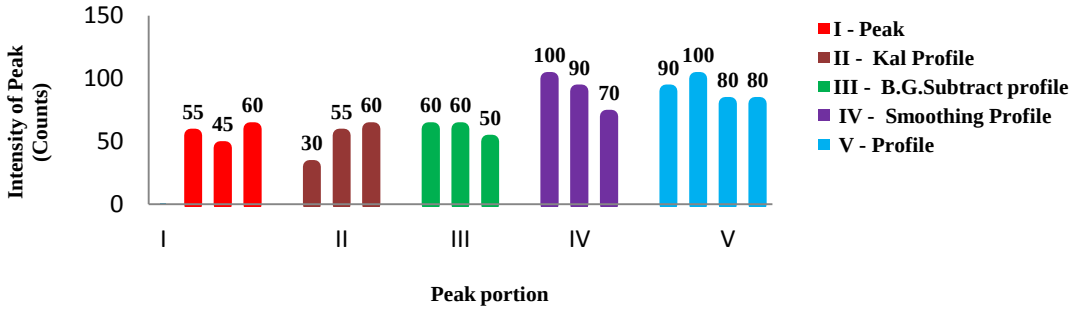

Figure 6: Intensity of Sodium Hydroxide in Geopolymer Concrete Sample

From the various portions of XRD graph, the intensity of sodium hydroxide of geopolymer concrete sample is plotted in a graph which is shown in Figure 6 From Figure 6, it is clear that the intensity of sodium hydroxide content of geopolymer concrete ranged from 30 counts to 100 counts. The V-profile exemplifies the intensity of silicon oxide about 70% more than the I-peak intensity. Also, the V-profile has 80% and 60% higher than the II-Kal profile and III-B. G. subtract profile intensities. Similarly, the V-profile has 4% increased value than IV-smoothing profile intensity. From these observations, it is proven that the sodium hydroxide content intensity increased only in IV-smoothing profile and V-profile portions and it attained maximum at profile portion only.

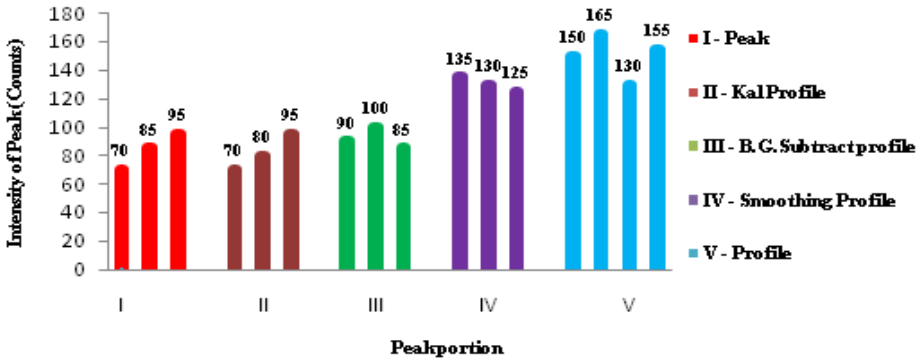

Figure 7: Intensity of Sodium Silicate in Geopolymer Concrete Sample

From the various portions of XRD graph, the intensity of sodium silicate of geopolymer concrete sample is plotted in a graph, shown in Figure 7. This indicates that the intensity of sodium silicate content of geopolymer concrete ranged from 70 counts to 165 counts. The V-profile points the intensity of silicon oxide about 90% more than the I-peak intensity. Also, the V-profile has 78% and 72% higher than the II-Kal profile and III-B. G. subtract profile intensities. Similarly, the V-profile has 21% increased value than IV-smoothing profile intensity. From these observations, it becomes clear that the sodium silicate content intensity increased only in IV-smoothing profile and V-profile portions and it attained the maximum at the profile portion only.

CONCLUSIONS

From the experimental investigations the following conclusions have been drawn

- The micro structural differences between fly ash and geopolymer concrete are readily visible by the SEM diagram.
- The diameter of the fly ash particles ranges from 10 to 200 micrometer and it is spherical in shape.
- The SEM image of the fly ash shows a dense state which indicates good alkali activation of fly ash.
- The SEM image of ordinary portland cement concrete shows that the microstructure of concrete is porous and not so dense.
- The SEM image of geopolymer concrete exposes the fully developed and compact microstructure which proves the complete polymerization process.
- In XRD analysis, the fly ash sample contains the silicon oxide at 2θ angle of 32° with the intensity of 600 counts.
- In geopolymer concrete sample, the sodium hydroxide chemical exists with an intensity of 100 counts at 2θ angle of 34° and at 36°.
- In geopolymer concrete sample, the sodium silicate reaches maximum with an intensity of 165 counts at 2θ angle of 32°.

REFERENCES

1. Davidovits, J. "Global Warming Impact on the Cement and Aggregates Industries", World Resource Review, Vol .6, No. 2, pp. 263-278, 1994.
2. Djwantoro Hardjito and Steenie, E. Wallah, "Development of Fly ash-based Geopolymer Concrete", ACI Materials Journal, Vol. 101, No. 6, pp. 467-472, 2004.
3. Douglas C. Comrie, John H. Paterson and Douglas J. Ritcey, "Applications of Geopolymer Technology to its stabilization", original paper, D.Comrie consulting Ltd, 120 Traders Boulevard east, Suite 209, Mississauga, Ontario, L4Z 2H7, pp. 161-165, 1998.
4. Fernandez Jimenez, A., Palomo, A. and Criado, M. "Microstructure development of alkali-activated fly ash cement: a descriptive model", Cement and Concrete Research, Vol. 34, No. 6, pp. 1204-1209, 2004.
5. Fernandez Jimenez, A.M. and De La Torre, A.G. "Quantitative determination of Phases in the alkali activation of fly ash Part I", Potential Ash Reactivity, Fuel, Vol. 85, No. 5-6, pp. 625-634, 2006.
6. Frantisek Skvara, Tomas Jilek and Lubomir Kopecky, "Geopolymer materials based on Fly ash", Ceramics Silika , Vol. 49, No. 3, pp. 195-204, 2005.
7. Frantisek Skvara, "Alkali activated materials or Geopolymers", Lecture notes, Department of Glass and Ceramics, Institute of Chemical Technology, Prague, pp. 173-177, 2007.
8. Jain, L.K. "Fly ash in cement and concrete: what experts say", The Indian Concrete Journal, Vol. 77, No.4, 2003.

9. Jo, B.W., Park, S.K. and Moon, R.G. "Properties of clinker-free mortar based on chemically bonded municipal solid iste incinerator ash", Magazine of Concrete Research, Vol. 60, No. 5, pp. 323-328, 2008.

10. Mehta, P.K. and Monteiro, P.J.M. "Concrete: Microstructure, Properties and Materials", Third Edition., McGraw Hill, New York, 2005.

11. Murhty, D.S.R., Venkata Ramesh, K. and Swarna Kumar, P. "Conservation of concrete-making materials", Journal of Structural Engineering, Vol. 33, No. 3, pp. 237-241, 2006.

12. Radhakrishna, A., Shashishankar and Udayashankar, B.C. "Analysis and assessment of strength development in class F fly ash based compressed geopolymer blocks", The Indian Concrete Journal, Vol. 82, No.5, pp. 31-37, 2008.

13. Raijiwala, D.B. and Patil, H.S. "Geopolymer concrete: A concrete of next decade", Journal of Engineering Research and Studies, Vol. II, No .2, pp. 19-25, 2011.